Full Length Article

Intermittent swelling and shrinkage of a highly expansive soil treated with polyacrylamide

Amin Soltani [a,*], An Deng [b], Abbas Taheri [b], Brendan C. O'Kelly [c]

[a] School of Engineering, Information Technology and Physical Sciences, Federation University, Churchill, VIC, 3842, Australia
[b] School of Civil, Environmental and Mining Engineering, The University of Adelaide, Adelaide, SA, 5005, Australia
[c] Department of Civil, Structural and Environmental Engineering, Trinity College Dublin, Dublin, D02 PN40, Ireland

A B S T R A C T

This laboratory study examines the potential use of an anionic polyacrylamide (PAM)-based material as an environmentally sustainable additive for the stabilization of an expansive soil from South Australia. The experimental program consisted of consistency limits, sediment volume, compaction and oedometer cyclic swell−shrink tests, performed using distilled water and four different PAM-to-water solutions of $P_D = 0.1$ g/L, 0.2 g/L, 0.4 g/L and 0.6 g/L as the mixing liquids. Overall, the relative swelling and shrinkage strains were found to decrease with increasing number of applied swell−shrink cycles, with an 'elastic equilibrium' condition achieved on the conclusion of four cycles. The propensity for swelling/shrinkage potential reduction (for any given cycle) was found to be in favor of increasing the PAM dosage up to $P_D = 0.2$ g/L, beyond which the excess PAM molecules self-associate as aggregates, thereby functioning as a lubricant instead of a flocculant; this critical dosage was termed 'maximum flocculation dosage' (MFD). The MFD assertion was discussed and validated using the consistency limits and sediment volume properties, both exhibiting only marginal variations beyond the identified MFD of $P_D = 0.2$ g/L. The accumulated axial strain progressively transitioned from 'expansive' for the unamended soil to an ideal 'neutral' state at the MFD, while higher dosages demonstrated undesirable 'contractive' states.

© 2022 Institute of Rock and Soil Mechanics, Chinese Academy of Sciences. Production and hosting by Elsevier B.V. This is an open access article under the CC BY-NC-ND license (http://creativecommons.org/licenses/by-nc-nd/4.0/).

1. Introduction

The design and implementation of linear infrastructure, such as pavements, are often negatively affected due to the presence of expansive clay formations (Soltani et al., 2020a). The term 'expansive' refers to the soils' vulnerability to seasonal moisture fluctuations, periodically expanding and contracting in volume, thereby adversely affecting the serviceability (and hence safety) of road infrastructure (Jones and Jefferson, 2012). To maintain engineering requirements, pavement engineers are often faced with a choice between (i) completing the design process within the limitations inflicted by the expansive subgrade, which mainly involves over-designing the upper pavement layers, or (ii) attempting to moderate the swell−shrink potential through soil stabilization. The latter is often preferred, since the former is not always financially

and/or logistically viable (Soltani et al., 2020b; Zhang et al., 2021). Unless successful, periodic maintenance may be required to preserve the end performance for either option.

Soil stabilization refers to the practice of altering a natural soil's structure, by physical and/or chemical alteration techniques, such that it is able to meet specific engineering requirements. Stabilization of expansive soils has been traditionally accomplished using calcium-based binders, particularly Portland cement and hydrated lime. The introduction of these agents to the soil−water complex initiates a course of short- and long-term chemical reactions, which encourage clay particle flocculation or aggregation, thereby leading to major improvements in critical soil attributes, such as shear strength/stiffness, load-bearing capacity, compressibility and swelling/shrinkage potential (e.g. Kalkan, 2011; Thyagaraj and Zodinsanga, 2014; Garzón et al., 2015; Al-Taie et al., 2020; Consoli et al., 2021). While effective from a stabilization perspective, calcium-based binders are not environmentally sustainable, as their application is commonly associated with substantial carbon emission footprints; this drawback highlights the urgency to minimize reliance on these binders (Ikeagwuani and Nwonu, 2019). A common solution in this context involves replacing calcium-

* Corresponding author.
E-mail address: a.soltani@federation.edu.au (A. Soltani).
Peer review under responsibility of Institute of Rock and Soil Mechanics, Chinese Academy of Sciences.

based materials with low-cost and more environmentally friendly ones. Promising alternatives, in terms of both geotechnical performance and sustainability, include polymers, resins and sulfonated oils (e.g. Mirzababaei et al., 2009; Yazdandoust and Yasrobi, 2010; Khatami and O'Kelly, 2013; Onyejekwe and Ghataora, 2015; James, 2020; Soltani et al., 2021).

Like calcium-based binders, the introduction of polymers to the soil—water medium can induce flocculation of the clay particles through relevant clay—polymer interaction mechanisms, i.e. charge neutralization, van der Waals or hydrogen bonding, and cationic bridging for cationic, neutral and anionic polymers, respectively (Theng, 1982; Ben-Hur et al., 1992). Among the multitude of commercially manufactured and readily available polymeric stabilizers, polyacrylamide (PAM) seems to possess a variety of favorable soil stabilization attributes and hence demands further attention. PAM refers to a group of synthetic polymers constructed from acrylamide (AMD) monomers ($CH_2 = CHC(O)NH_2$); they are hydrophilic (and hence water-soluble) in nature and can be synthesized in anionic, neutral or cationic forms (Seybold, 1994). PAM-based agents have been successfully employed within a variety of industries, including their application as a flocculant in sludge dewatering and water treatment processes, as well as their adoption in the agricultural sector to increase the soil—water retention capacity under drought conditions (e.g. Orts et al., 2007; Xiong et al., 2018; Chang et al., 2020). In the geotechnical context, reported applications for PAM include dewatering of mine tailings, increasing soil compaction efficiency, mitigating desiccation-induced cracking in clays, for shear strength enhancement and seepage/erosion control (e.g. Lei et al., 2018; Soltani et al., 2019a; Soltani-Jigheh et al., 2019; Zhang et al., 2019; Georgees and Hassan, 2020; Kou et al., 2021). Though promising, the results reported by these studies, especially for expansive clays, are still limited (and somewhat inconsistent) to warrant PAM as an *ad hoc* soil-stabilization scheme. Moreover, to the authors' knowledge, the available data on PAM-treated soils have been mainly limited to certain routine geotechnical laboratory tests, which, though valuable, have not been sufficient so far as to provide the confidence needed to promote PAM-based materials for widespread usage in soil stabilization projects. In the expansive soil context, for instance, a full review of the existing literature shows that the swell—shrink volume change potential of PAM-treated expansive soils when subjected to intermittent wetting and drying, as would be the case for field conditions, has not yet been investigated, thus implying the need for further research to better understand PAM's durability and hence its true stabilization potentials and/or limitations.

This laboratory study examines the potential use of an anionic PAM-based material as an environmentally sustainable material for the stabilization of an expansive soil from South Australia. The primary objectives are to investigate the effects of PAM treatment, at different PAM-to-water (mass-to-volume) dosages, on the soil's consistency, sedimentation, compactability, and swell—shrink volume change behaviors. The principles of soil chemistry are then combined with the soil mechanics framework to identify and discuss the clay—PAM amending interactions in the context of cyclic swelling and shrinkage.

2. Test materials

2.1. Test soil

The soil selected for this experimental investigation was a reddish-brown clay material sourced from a site near Adelaide, South Australia. Table 1 summarizes the main physical and mechanical properties of the test soil. In terms of texture, the soil contained 20% sand (0.075—4.75 μm), 36% silt (2—75 μm) and 44%

Table 1
Physical and mechanical properties of the test soil.

Property classification	Soil property	Value	Standard designation
Particle-size distribution (PSD)	Coarse sand fraction (2—4.75 mm) (%)	1	ASTM D422-63(2007)e2 (2007)
	Medium sand fraction (0.425—2 mm) (%)	4	ASTM D422-63(2007)e2 (2007)
	Fine sand fraction (0.075—0.425 mm) (%)	15	ASTM D422-63(2007)e2 (2007)
	Silt fraction (2—75 μm) (%)	36	ASTM D422-63(2007)e2 (2007)
	Clay fraction (<2 μm) (%)	44	ASTM D422-63(2007)e2 (2007)
Atterberg limits	Fall-cone liquid limit, LL (%)	78	AS 1289.3.9.1 (2015)
	Rolling-thread plastic limit, PL (%)	22.4	AS 1289.3.2.1 (2009)
	Plasticity index, $PI = LL - PL$ (%)	55.6	—
	Linear shrinkage, LS (%)	15.8	AS 1289.3.4.1 (2008)
Swelling properties	Swelling potential, P_{SW} (%)[a]	10.7	ASTM D4546-14 (2014)
	Swelling pressure, σ_{SW} (kPa)[b]	235	ASTM D4546-14 (2014)
	Free swell ratio, FSR	2.27	Prakash and Sridharan (2004)
Classifications	USCS soil classification	CH	ASTM D2487-17 (2017)
	Principal clay mineral	Montmorillonite	Prakash and Sridharan (2004)
	Degree of expansivity (based on P_{SW})	High	Seed et al. (1962)
	Degree of expansivity (based on FSR)	High	Prakash and Sridharan (2004)
Standard Proctor (SP) compaction characteristics	Specific gravity, G_s	2.76	ASTM D854-14 (2014)
	Optimum moisture content (OMC), w_{opt} (%)	20.2	ASTM D698-12 (2012)
	Maximum dry unit weight (MDUW), γ_{dmax} (kN/m³)	15.9	ASTM D698-12 (2012)
	Void ratio at MDUW, e^c	0.702	ASTM D698-12 (2012)

[a] Ultimate axial swelling strain for the SP-compacted sample under a 7-kPa surcharge.
[b] Swelling pressure for the SP-compacted sample determined by the 'loading-after-wetting' test scheme (i.e. Method C in ASTM D4546-14 (2014)).
[c] Calculated by $e = G_s\gamma_w/\gamma_{dmax} - 1$ (where γ_w is the unit weight of water).

clay (<2 μm), as per ASTM D422-63(2007)e2 (2007). The liquid limit (LL), obtained using a standard 80 g—30° fall-cone device for a cone penetration depth at the LL of 20 mm (AS 1289.3.9.1, 2015), and the rolling-thread plastic limit (PL) (AS 1289.3.2.1, 2009) were obtained as $LL = 78\%$ and $PL = 22.4\%$; hence, producing a plasticity index ($PI = LL - PL$) value of 55.6% (see Table 1). Note that the described fall-cone definition for LL and the testing method for PL are different from those specified in the Chinese testing standard JTG E40-07 (2007), *Test Methods of Soils for Highway Engineering*, whereby the fall-cone approach is employed for PL as well as LL determinations; with a discussion on these aspects and their implications presented in the paper by Vardanega et al. (2020). In view of its fines content (<75 μm) of 80%, along with its measured LL and PI values, the test soil can be graded as clay with high

plasticity (CH) based on the unified soil classification system (USCS) (ASTM D2487-17, 2017).

The maximum dry unit weight (MDUW) and optimum moisture content (OMC), determined for the standard Proctor (SP) compaction test (ASTM D698-12, 2012), were measured as 15.9 kN/m^3 and 20.2%, respectively. The swelling potential (P_{SW}) for the SP-compacted soil sample, defined as the sample's ultimate axial swelling strain measured using an oedometer set-up for an applied surcharge of 7 kPa (ASTM D4546-14, 2014), was found to be 10.7%. According to the P_{SW}-based classification framework (Seed et al., 1962), the test soil is classified as highly expansive. The free swell ratio (FSR) is defined as the ratio of equilibrium sediment volume of 10 g oven-dried soil (<425 μm) in distilled water to that in kerosene (Prakash and Sridharan, 2004). According to the FSR-based classification framework (Prakash and Sridharan, 2004), linking the FSR value to the type of principal clay mineral present in fine-grained soils, it can be concluded that the clay fraction of the test soil was mainly dominated by montmorillonite.

2.2. PAM-based stabilizer

A proprietary anionic PAM-based material, similar to that examined by Soltani et al. (2018, 2019a) and Zhang et al. (2021), was used as the soil-stabilizing agent. Referring to Fig. 1a, the product was supplied in granular form and, as per the manufacturer's instructions, was to be diluted with water for application. In terms of charge development, the anionic character (see Fig. 1b) can be established through two common pathways (Barvenik, 1994): (i) copolymerization of AMD and acrylic acid (CH$_2$ = CHCOOH) or a salt of acrylic acid, and (ii) hydrolysis of the neutral PAM with sodium hydroxide (NaOH) or a similarly strong base. As reported in the manufacturer's literature, the PAM-based material possessed a neutral pH value of 6.9 (at 25 °C), a specific gravity of 0.8, a rather high molecular weight ranging between 12 Mg/mol and 15 Mg/mol (i.e. equivalent to approximately 1.5×10^5 monomer units per PAM molecule), and a moderate density charge of approximately 18%.

3. Experimental work

3.1. Soil—PAM mix designs and preliminary tests

The primary objective of this experimental study is to examine the effects of PAM treatment on the soil's consistency, sedimentation, compactability, and swell—shrink volume change behaviors. Accordingly, five soil—PAM mix designs (i.e. unamended soil and four PAM-treated blends) were examined. For the PAM-treated cases, PAM solutions with dosages (i.e. mass of granular PAM to volume of distilled water) of P_D = 0.1 g/L, 0.2 g/L, 0.4 g/L and 0.6 g/L were prepared as the mixing liquids, which were used in wetting the dry soil to the required moisture contents for forming the various test samples. For ease of presentation, the unamended soil and the four PAM-treated blends (with P_D = 0.1 g/L, 0.2 g/L, 0.4 g/L and 0.6 g/L) are designated as P0, P1, P2, P4 and P6, respectively.

The preliminary tests included consistency limits (AS 1289.3.2.1, 2009; AS 1289.3.9.1, 2015), sediment volume (Prakash and Sridharan, 2004) and SP compaction (ASTM D698-12, 2012) tests, performed using distilled water (for P0) and different PAM solutions (for P1, P2, P4 and P6) as the mixing liquid. The primary testing stage investigated the oedometer cyclic swell—shrink behavior (see Section 3.2) of SP-compacted samples for each of the considered mixing liquids. In preparing these samples, the unamended and PAM-treated soils prepared at their respective OMCs were statically compacted in three equal-height layers into a series of confining rings (height = 20 mm and diameter = 50 mm), such that each layer achieved its respective MDUW (values are presented and discussed in Section 4.3). To ensure even moisture distribution throughout the sample volume, a 24-h standing period, during which the compacted samples were hermetically sealed and stored at ambient laboratory temperature, occurred between static compaction and commencement of the oedometer test.

3.2. Oedometer cyclic swell—shrink tests

The SP-compacted unamended soil and various PAM-treated samples were exposed to intermittent swelling and shrinkage processes in a temperature-controlled oedometer apparatus, as employed previously in Soltani et al. (2019b, 2021). The samples placed within the oedometer cell were inundated with distilled water and allowed to freely swell under an applied 7-kPa surcharge (ASTM D4546-14, 2014), at ambient laboratory temperature, to a point at which the axial swelling strain achieved a stabilized state (i.e. completion of the primary swelling phase). The strain corresponding to this state is referred to as the 'swelling potential'. In performing the subsequent shrinkage stage, the inundation water was first drained away via a drainage valve fitted to the base of the oedometer cell. Next, the cell's external heating component was set to a temperature of (40 ± 2) °C, causing the samples to shrink (while still subjected to the same applied 7-kPa surcharge). Shrinkage was carried on to a point at which the ultimate axial shrinkage strain (i.e. completion of the normal/primary shrinkage phase), referred to as the 'shrinkage potential', could be obtained. Intermittent wetting and drying of the samples were replicated in a similar fashion, with the combination of one swelling stage and the following shrinkage process being defined as one swell—shrink cycle. The swelling and shrinkage potentials have been reported
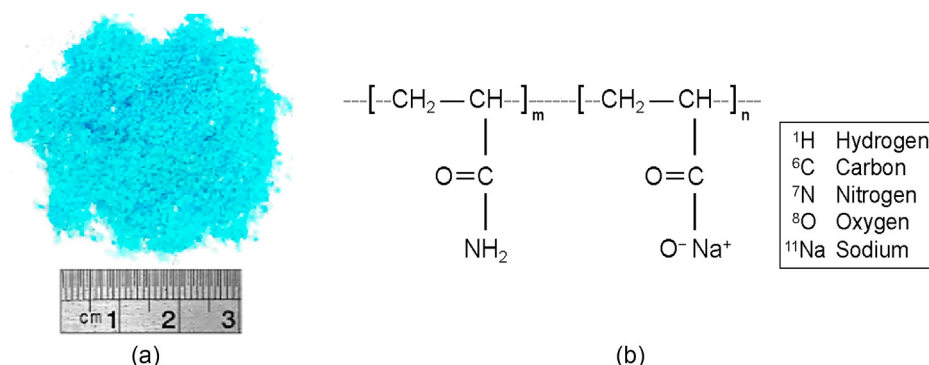

Fig. 1. (a) Anionic PAM in its granular form, and (b) Structural formula of anionic PAMs.

to equalize on the conclusion of several cycles (Subba Rao, 2000; Tripathy et al., 2002). In the present investigation, the swell–shrink equilibrium condition was mainly attained on the conclusion of four cycles; as such, the test samples were exposed to a maximum of six cycles. The relative swelling and shrinkage potentials (for any given cycle) were calculated as follows (Soltani et al., 2019c):

$$P_{SW}(N) = \frac{\Delta H_{SW}(N)}{H_{SH}(N-1)} \times 100\%$$ (1)

$$P_{SH}(N) = \frac{\Delta H_{SH}(N)}{H_{SW}(N)} \times 100\%$$ (2)

where $P_{SW}(N)$, $H_{SW}(N)$ and $\Delta H_{SW}(N)$ are the swelling potential, sample height and increase in sample height, respectively, on conclusion of the Nth swelling cycle; $P_{SH}(N)$ and $\Delta H_{SH}(N)$ are the shrinkage potential and decrease in sample height, respectively, on conclusion of the Nth shrinkage cycle; and $H_{SH}(N-1)$ is the sample height on conclusion of the $(N-1)$th shrinkage cycle.

4. Results and discussion

4.1. Effect of PAM treatment on soil consistency behavior

Fig. 2a illustrates the variations of the soil consistency limits against PAM dosage P_D for the tested mix designs. The soil–PAM
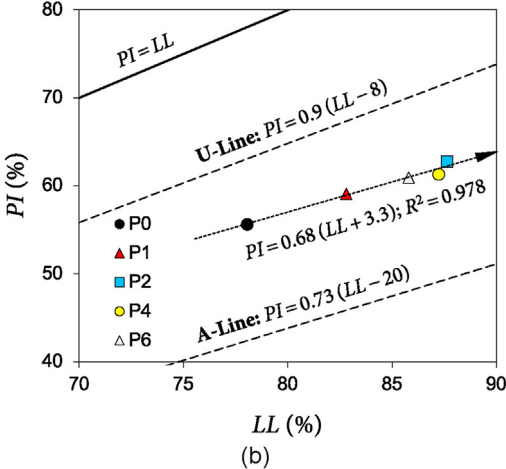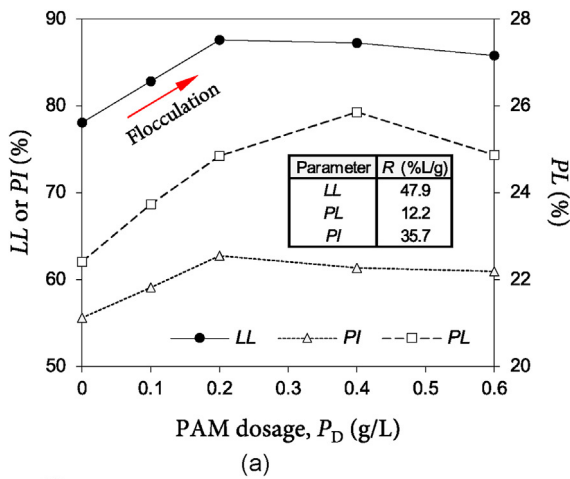

Fig. 2. Effect of PAM treatment on the test soil's consistency limits: (a) Variations of the LL, PL and PI against PAM dosage P_D; and (b) The tested mix designs plotted on the Casagrande-style PI–LL chart.

mixtures (P1, P2, P4 and P6) all had higher LL, PL and PI values compared to those measured for the unamended soil (P0). The greater the PAM dosage, the higher the LL, PL and PI parameters up to $P_D = 0.2$ g/L, beyond which only marginal variations occurred. From Fig. 2a, the rates of increase in the consistency indices with respect to $P_D \leq 0.2$ g/L, defined as the slopes of linear trendlines fitted through the LL–P_D, PL–P_D and PI–P_D datasets, were calculated as $R = 47.9\%$ L/g, 12.2% L/g, and 35.7% L/g, respectively, where R represents the rate of increase in the consistency parameters with respect to $P_D \leq 0.2$ g/L.

Fig. 2b illustrates the tested mix designs when represented on the Casagrande-style soil plasticity chart, with all mixtures plotting between the A- and U-lines, thereby indicating that the unamended soil and its various PAM-based blends categorize as clay materials. Despite the PAM addition causing a considerable rightward–upward translation in the PI–LL space, the original CH classification of the unamended soil remained valid for all PAM-treated cases. The PI–LL relationship for these materials was found to be linear (somewhat parallel to the A-line), according to the expression $PI = 0.68 (LL + 3.3)$ (with $R^2 = 0.978$).

The LL can be considered as a guide towards perceiving soil fabric evolution in response to changes in pore-water chemistry (Sivapullaiah, 2015; Muguda and Nagaraj, 2019). During the fall-cone LL test, as clay particle flocculation begins to dominate the soil matrix, the resistance to penetration by the fall-cone (and hence shear strength) increases; as such, the cone penetration depth criteria for LL determination will be achieved at higher moisture contents (Kim and Palomino, 2009; Soltani et al., 2019a). Accordingly, one can postulate that an increase in the LL, as achieved by PAM treatment, signifies an increased tendency for clay particle flocculation. On this basis, the maximum flocculation tendency appears to be attained at 0.2 g/L PAM, since higher dosages did not produce notable further increases in the LL. Moreover, the hydrophilic character of PAM molecules may provide extra adsorption sites (in addition to the clay particles) for water molecules, thereby further contributing towards higher consistency limits for soil–PAM mixtures (Kim and Palomino, 2009; Soltani-Jigheh et al., 2019).

4.2. Effect of PAM treatment on soil sedimentation behavior

Results of the sediment volume tests are shown in Fig. 3. The soil–PAM suspensions (P1, P2, P4 and P6) all produced lower equilibrium sediment volumes compared to that of the soil–water suspension (P0). The equilibrium sediment volume was found to follow an exponentially-decreasing trend with increasing PAM dosage; only minor added benefits/reductions were noted beyond 0.2 g/L PAM. The soil–water suspension resulted in a relatively high equilibrium sediment volume of $V_{SD} = 34$ mL, while the PAM-treated suspensions with $P_D = 0.1$ g/L, 0.2 g/L, 0.4 g/L and 0.6 g/L had lower values of $V_{SP} = 28.5$ mL, 25 mL, 24.5 mL, and 23 mL, respectively. With the soil–kerosene suspension having an equilibrium sediment volume of $V_{SK} = 15$ mL, the FSR parameter, calculated as $FSR = V_{SD}/V_{SK}$ (for P0) or V_{SP}/V_{SK} (for PAM-treated cases), can be calculated as 2.27, 1.9, 1.67, 1.63, and 1.53 for P0, P1, P2, P4 and P6, respectively, where V_{SD}, V_{SP} and V_{SK} are the equilibrium sediment volumes of 10 g oven-dried soil (<425 μm) in distilled water (the 'polar' liquid), PAM solution and kerosene (the 'non-polar' liquid), respectively.

From the FSR-based classification framework presented in Table 2 (Prakash and Sridharan, 2004), the unamended soil is classified as highly expansive, while all PAM-treated cases produced an improved classification of moderately expansive. Like the LL, the FSR can be used to infer, and hence predict, the evolution of soil fabric (Sridharan and Prakash, 1999; Soltani et al., 2018). A
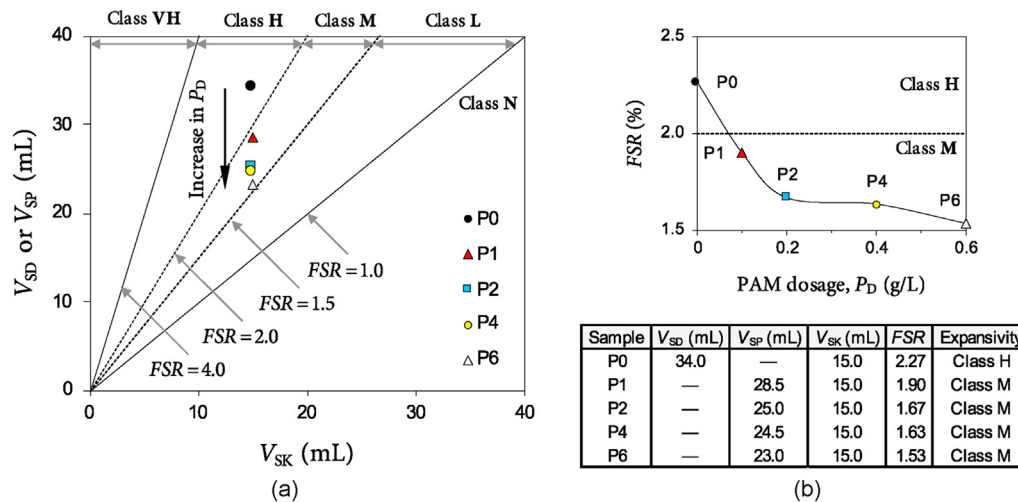
Fig. 3. Effect of PAM treatment on the test soil's sedimentation properties: (a) Equilibrium sediment volume measurements; and (b) Variations of the *FSR* against PAM dosage P_D.

decrease in the *FSR*, as achieved by suspending the soil in PAM solution, indicates an increased tendency for clay particle flocculation; this hinders the clay particles from expanding to their full potential, which would have otherwise occurred in distilled water (Kim and Palomino, 2009; Soltani et al., 2019a). Like the $LL–P_D$ relationship (see Section 4.1), the maximum tendency for flocculation, based on the *FSR* results, appears to also be attained at $P_D = 0.2$ g/L, with higher PAM dosages not providing notable further improvements (or reductions) in V_{SP} and hence by association the *FSR*.

4.3. Effect of PAM treatment on soil compactability behavior

Typical SP compaction curves for the mixtures P0, P2 and P6 are shown in Fig. 4, with the complete test results presented in Table 3. The compaction curve experienced a considerable upward translation for the addition of (and dosage increase in) PAM, hence improving the soil's compactability. While marked increases were noted for the MDUW (increasing from 15.9 kN/m³ for the unamended soil to 16.1 kN/m³, 16.3 kN/m³, 16.4 kN/m³, and 16.7 kN/m³ for the mixtures P1, P2, P4 and P6, respectively), the corresponding OMC values exhibited negligible changes (follow the arrowed line in Fig. 4).

An increase in pore-water viscosity, which is the case when employing PAM solutions (in lieu of distilled water) as the compaction liquid, induces inter-particle lubrication. Consequently, the movement of the soil agglomerations (and clay flocs) relative to each other during compaction is confronted with much less friction (Onyejekwe and Ghataora, 2015; Soltani et al., 2021). This mechanism allows a relatively denser packing of the soil particles to be obtained for the same compactive energy, which produces higher MDUW values for the soil–PAM mixtures.

The OMC and MDUW parameters are often estimated using rolling-of-threads *PL* measurements. Two of the more common, yet simple, correlations in this context are given as follows (Gurtug and Sridharan, 2002, 2004):

$$w_{opt}^P = \beta_M PL \tag{3}$$

$$\gamma_{dmax}^P = \beta_D \gamma_{dP} = \frac{\beta_D G_s \gamma_w}{1 + G_s PL} \tag{4}$$

where w_{opt}^P is the predicted OMC, γ_{dmax}^P is the predicted MDUW, γ_{dP} is the dry unit weight at the *PL* (determined by the rolling-thread method), and β_M and β_D are the empirical coefficients (dimensionless).

The empirical coefficients β_M and β_D are functions of the compaction energy level. For typical fine-grained soils and the SP compaction energy, they can be taken as $\beta_M = 0.92$ and $\beta_D = 0.98$ (Gurtug and Sridharan, 2004). Comparing the experimental results and empirical predictions presented in Table 3, the routine practice of interpreting the compaction characteristics using rolling-of-threads *PL* measurements cannot be reliably extended to PAM-treated soils (i.e. $R^2 = 0.086$ and 0.654 for the OMC and MDUW predictions, respectively).

4.4. Effect of PAM treatment on soil cyclic swell–shrink behavior

4.4.1. Relative swelling and shrinkage potentials

The evolution of the swelling potential P_{SW} (see Eq. (1)) with respect to the number of imposed swell–shrink cycles N is shown in Fig. 5a. For the samples P0 and P1, the $P_{SW}–N$ relationship demonstrated a rise–fall trend, peaking at $N = 2$ and then decreasing exponentially up to the fourth (or equilibrium) cycle, beyond which only marginal reductions occurred (follow the trend curves 'P0' and 'P1' in Fig. 5a). Meanwhile, the $P_{SW}–N$ relationship for the samples P2, P4 and P6 exhibited an exponentially-decreasing trend. Overall, for any given cycle, the greater the PAM dosage, the lower the developed swelling potential; compared to 0.2 g/L PAM, however, the relative reductions in the swelling potential for $P_D = 0.4$ g/L and 0.6 g/L were noticeably small (e.g. compare the trend curves 'P2' and 'P6' in Fig. 5a). For instance, at $N = 3$, the samples P0, P1, P2, P4 and P6 resulted in $P_{SW} = 9.6\%$, 7.7%, 4.2%, 3.5% and 3.3%, respectively. The degree of expansivity for the investigated mix designs was assessed using the three P_{SW}-based classification frameworks summarized in Table 4 (Holtz and Gibbs, 1956; Seed et al., 1962; Sridharan and Prakash, 2000). From the final results presented in Table 5, compared to the highly expansive classification of the test soil, the expansivity classifications were either maintained ($N = 1$) or substantially improved ($N \geq 2$) for all PAM dosages, especially for $P_D \geq 0.2$ g/L.

Fig. 5b shows the variations of the shrinkage potential P_{SH} (see Eq. (2)) against the number of applied cycles. For any given PAM dosage, the shrinkage potential followed an exponentially-

Table 2
Classification procedures for expansive soils based on the *FSR* parameter (Prakash and Sridharan, 2004).

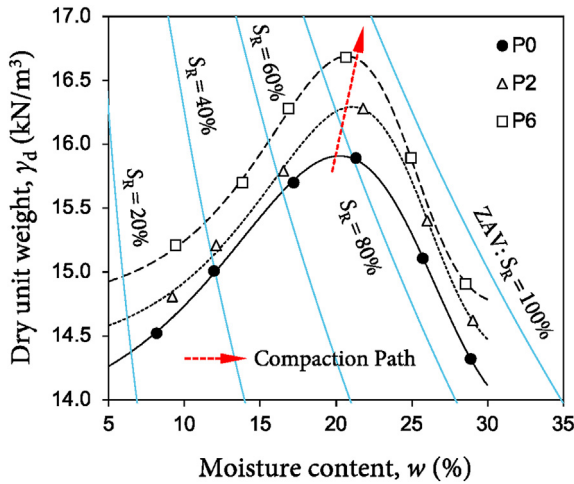| $FSR = V_{SD}/V_{SK}$	Expansivity level class	Principal clay mineral
≤1	Negligible (class N)	Kaolinite
1—1.5	Low (class L)	Kaolinite + montmorillonite
1.5—2	Moderate (class M)	Montmorillonite
2—4	High (class H)	Montmorillonite
>4	Very high (class VH)	Montmorillonite

Fig. 4. Typical SP compaction curves for the unamended soil (P0) and soil—PAM mixtures containing 0.2 g/L and 0.6 g/L PAM (P2 and P6). Note that ZAV denotes zero-air-voids (saturation degree $S_R = 100\%$).

Table 3
Summary of the SP compaction characteristics for the tested samples.

Sample	Measured OMC (%)	Measured MDUW (kN/m³)	PL (%)	Predicted OMC, w_{opt}^{P} (%)[a]	Predicted MDUW, γ_{dmax}^{P} (kN/m³)[b]
P0	20.2	15.9	22.4	20.6	16.4
P1	20.3	16.1	23.7	21.8	16
P2	21.1	16.3	24.9	22.9	15.7
P4	20.2	16.4	25.9	23.8	15.5
P6	20.7	16.7	24.9	22.9	15.7

[a] Calculated by Eq. (3) with $\beta_M = 0.92$.
[b] Calculated by Eq. (4) with $\beta_D = 0.98$.

exchange capacity and accordingly its volume change potential. Further, the formation and diffusion of these strong cationic bridges between adjacent clay surfaces (which bring and hold the clay particles together) induce flocculation of the clay particles, thus decreasing the soil's swell—shrink tendency. The maximum tendency for flocculation, however, would be limited by the number of attraction sites (i.e. the soil clay content) and the amount of exchangeable divalent cations available for the PAM molecules (Latifi et al., 2016; Soltani et al., 2021). In other words, for a given soil type, beyond a critical PAM dosage, for which the available attraction sites are exhausted, the flocculation process will cease. Increasing the PAM dosage beyond this so-called 'maximum flocculation dosage' (MFD) may cause the excess PAM molecules to self-associate as aggregates, thereby functioning as a lubricant instead of a flocculant (Soltani et al., 2019a). Accordingly, an increase in PAM dosage beyond the soil's MFD should not provide further notable improvements in the soil's mechanical properties. This mechanism explains the marginal variations observed in the consistency limits (see Fig. 2), sediment volume features (see Fig. 3), and swell—shrink volume changes (see Fig. 5) for $P_D > 0.2$ g/L, implying for the present investigation that MFD equals 0.2 g/L.

Referring to Fig. 5, overall, the swelling and shrinkage potentials decreased with increasing number of applied swell—shrink cycles. This behavior, as reported by previous researchers (e.g. Subba Rao,
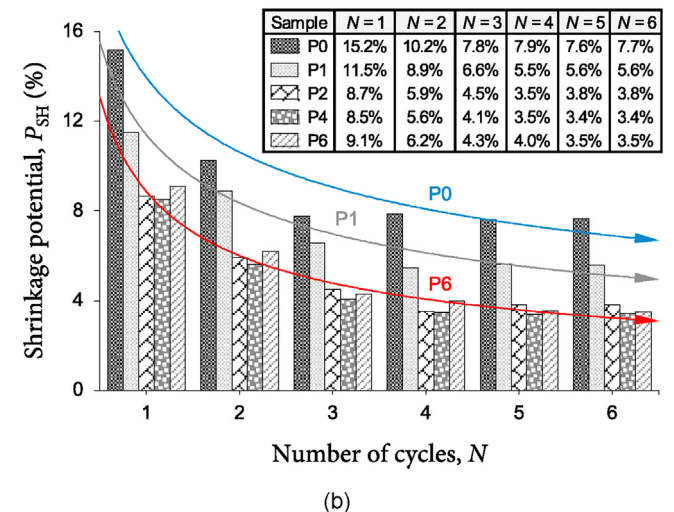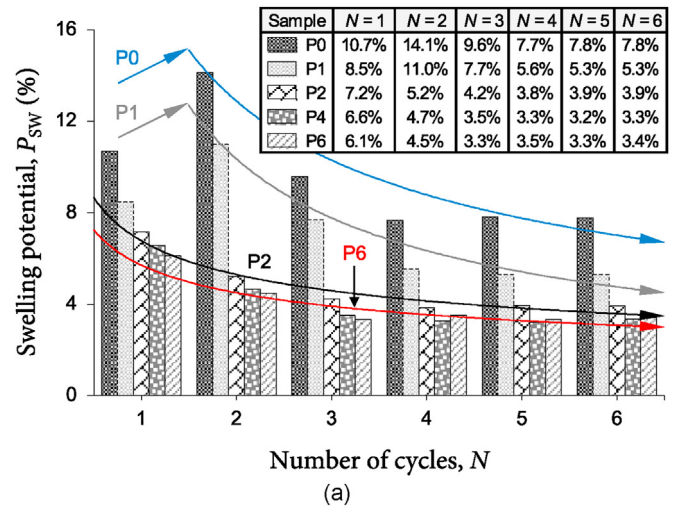

(a)

(b)

Fig. 5. Variations of (a) swelling and (b) shrinkage potentials (i.e. P_{SW} and P_{SH}) against the number of applied swell—shrink cycles N for the tested samples.

decreasing trend for an increasing number of applied cycles, with negligible reductions occurring beyond the equilibrium cycle ($N = 4$). Like the swelling potential, for any given cycle, the propensity for shrinkage potential reduction was in favor of increasing the PAM dosage up to $P_D = 0.2$ g/L, beyond which the observed reductions became marginal, with the trend curves for the samples P2, P4 and P6 observed to overlap with each other. For instance, at $N = 3$, the samples P0, P1, P2, P4 and P6 resulted in $P_{SH} = 7.8\%$, 6.6%, 4.5%, 4.1% and 4.3%, respectively.

Clay particles carry an unbalanced negative charge, such that they would naturally repel the anionic PAM molecules (owing to electrostatic repulsions). However, clay—PAM attractions can still be developed through the cationic bridging mechanism, explained as follows. Exchangeable cations present near the clay particle surfaces, particularly divalent cations such as Ca^{2+} and Mg^{2+}, function as 'attraction bridges' between the negatively charged clay and PAM components (Seybold, 1994; Laird, 1997; Lu et al., 2002; Soltani et al., 2018; Georgees and Hassan, 2020). This immobilizes the exchangeable cations near the clay surfaces, decreasing the soil's overall cation-

Table 4
Classification procedures for expansive soils based on the P_{SW} parameter.

Expansivity level class	Ultimate axial swelling strain, P_{SW} (%)		
	Holtz and Gibbs (1956)[a]	Seed et al. (1962)[b]	Sridharan and Prakash (2000)[a]
Low (class L)	<10	0–1.5	1–5
Moderate (class M)	10–20	1.5–5	5–15
High (class H)	20–30	5–25	15–25
Very high (class VH)	>30	>25	>25

Note: Ultimate axial swelling strain of [a] an air-dried SP-compacted sample and [b] an SP-compacted sample, both under a 7-kPa surcharge.

2000; Zhang et al., 2006; Estabragh et al., 2015; Soltani et al., 2019c; Estabragh et al., 2020), can be ascribed to the reconstruction of the soil/soil–PAM microstructures on completion of the second (for P0 and P1) or first (for P2, P4 and P6) drying cycle. As the moisture content decreases during drying, capillary stresses begin to rise due to an increased surface tension leading strong van der Waals bonds to form and propagate between adjacent soil particles (and clay flocs), causing them to aggregate. This change in soil fabric leads to an apparent reduction in the sample's clay content, consequently decreasing its overall water adsorption–retention capacity and its volume change potential during subsequent cycles.

4.4.2. Cumulative swell–shrink patterns

For any given cycle, the accumulated axial strain, given as the sum of the axial plastic strain (APS) values up to that cycle, can be calculated as follows (Zhao et al., 2019; Soltani et al., 2021):

$$\varepsilon_{ac}(N) = \begin{cases} \sum_{N=1}^{6}[P_{SW}(N) - P_{SH}(N-1)] \text{ (for SW)} \\ \sum_{N=1}^{6}[P_{SW}(N) - P_{SH}(N)] \text{ (for SH)} \end{cases} \quad (5)$$

where $\varepsilon_{ac}(N)$ is the accumulated axial strain on conclusion of the Nth swelling (for SW) or shrinkage (for SH) cycle (in %); $P_{SW}(N)$ is the relative swelling potential on conclusion of the Nth swelling cycle (obtained by Eq. (1), as %); and $P_{SH}(N-1)$ and $P_{SH}(N)$ are the relative shrinkage potentials on conclusion of the $(N-1)$th and Nth shrinkage cycles, respectively (obtained by Eq. (2), as %).

Fig. 6 illustrates the ε_{ac}–N relationship (see Eq. (5)), referred to as the swell–shrink rhythm/pattern, for the tested mix designs. As per common practice, for each of the tested samples, the accumulated axial strain was interpreted (in terms of character and extent) using the slope of a single-coefficient trendline fitted to the sample's respective swell–shrink rhythm (Soltani et al., 2019b):

$$\varepsilon_{ac} = \lambda N \quad (6)$$

where λ is the trendline slope (in %). Based on the sign and magnitude of λ, the following three cases can be postulated:

(1) Expansive: Positive values of λ indicate that the net extent of the developed P_{SW} strains is greater than that of the P_{SH} strains (i.e. $\Sigma P_{SW} > \Sigma P_{SH}$). As such, the ε_{ac} parameter bears an undesirable expansive character, with higher values of λ indicative of more extreme free-surface ground heave.

(2) Neutral: For those cases where λ is equal (or fairly close) to zero, one can postulate that $\Sigma P_{SW} \approx \Sigma P_{SH}$. In other words, the ε_{ac} parameter is neutral in character, with this case considered ideal in terms of minimizing free-surface ground movements.

(3) Contractive: Negative values of λ indicate that $\Sigma P_{SW} < \Sigma P_{SH}$; thus, the ε_{ac} parameter is contractive in character. Like the expansive case, this case is also undesirable, with higher absolute values of λ producing more extreme free-surface ground settlements.

Referring to Fig. 6, relative to the expansive deformational state of the unamended soil (P0 with $\lambda = 1.1\%$), the ε_{ac}–N relationship for the treated soil underwent a progressive downward translation with increasing PAM dosage. The samples P1 and P2 produced lower λ values of 0.62% and −0.04%, respectively, signifying a progressive transition towards the ideal neutral case at $P_D = 0.2$ g/L. Higher PAM dosages of 0.4 g/L and 0.6 g/L produced highly pronounced negative λ values of −0.44% and −0.99%, respectively, both indicative of an undesirable contractive condition. In view of these findings, as well as the relative P_{SW} and P_{SH} strain responses presented in Fig. 5, the 0.2 g/L PAM dosage (which also happens to represent the soil's MFD) can be deemed as the optimum dosage to minimize swell–shrink induced heave and settlements.

The incurred APS, described as the algebraic difference of the relative P_{SW} and P_{SH} strains for a given cycle (e.g. see the double arrowed line 'APS' for P0 at $N = 2$ in Fig. 6a), decreased with increasing number of applied cycles and substantially diminished on the conclusion of four cycles. In other words, the relative P_{SW} and P_{SH} strains became elastic in character for $N \geq 4$. Thus, on achieving swell–shrink equilibrium, the P_{SW} and P_{SH} strains for each tested sample develop into their unique and interchangeable value, commonly referred to as the equilibrium bandwidth (EB) (Subba Rao, 2000; Tripathy et al., 2002; Yazdandoust and Yasrobi, 2010). As shown in Fig. 6, the greater the PAM dosage, the lower the EB value; however, compared with that for $P_D = 0.2$ g/L (i.e. the MFD), the relative reductions in the EB for 0.4 g/L and 0.6 g/L PAM were marginal. The unamended soil (P0) produced an EB value of 7.7%, while the samples P1, P2, P4 and P6 resulted in lower values of 5.6%, 3.8%, 3.4% and 3.5%, respectively.

As discussed earlier, beyond the soil's MFD of 0.2 g/L, the PAM material's lubricant features may begin to dominate its flocculant properties. Consequently, where swell–shrink equilibrium has not yet been achieved (for $N < 4$), the movement of the soil agglomerations (and clay flocs) relative to each other, under the applied 7-kPa surcharge in these tests, would be confronted with less friction (particularly for $P_D >$ MFD). This allows a denser packing of the soil particles to be obtained during drying, thereby potentially increasing the sample's shrinkage-to-swelling (P_{SH}/P_{SW}) ratio and hence decreasing its ε_{ac}–N trendline slope λ. To examine this hypothesis, a scatter plot showing the variations of P_{SH}/P_{SW} against the number of imposed swell–shrink cycles is presented in Fig. 7. Overall, the greater the PAM dosage, the higher the P_{SH}/P_{SW} ratio, particularly evident for $N = 2$–4, which elucidates the relatively larger contractive character of the samples P4 and P6 compared to those containing $P_D \leq$ MFD. Accordingly, it can be concluded that, while PAM dosages greater than the MFD produce similar improvement effects to those achieved at the MFD, they may exhibit higher P_{SH}/P_{SW} ratios during early cycles. As such, in addition to higher costs, PAM dosages greater than the MFD may be associated with potentially major settlement concerns. One can postulate that such concerns would tend to intensify as the applied surcharge (overburden stress) increases, which is a critical aspect that demands further examination.

5. Conclusions

This laboratory study examined the potential use of an anionic PAM-based material, employed at four PAM-to-water (mass-to-volume) dosage ratios of $P_D = 0.1$ g/L, 0.2 g/L, 0.4 g/L, and 0.6 g/L, for

Table 5
Degree of expansivity for the tested samples during various swelling cycles.

| Sample	Degree of expansivity					
	$N=1$	$N=2$	$N=3$	$N=4$	$N=5$	$N=6$
P0	High[a]	Moderate[b]	Low[b]	Low[b]	Low[b]	Low[b]
		Moderate[c]	Moderate[c]	Moderate[c]	Moderate[c]	Moderate[c]
P1	High[a]	Moderate[b]	Low[b]	Low[b]	Low[b]	Low[b]
		Moderate[c]	Moderate[c]	Moderate[c]	Moderate[c]	Moderate[c]
P2	High[a]	Low[b]	Low[b]	Low[b]	Low[b]	Low[b]
		Moderate[c]	Low[c]	Low[c]	Low[c]	Low[c]
P4	High[a]	Low[b]	Low[b]	Low[b]	Low[b]	Low[b]
		Low[c]	Low[c]	Low[c]	Low[c]	Low[c]
P6	High[a]	Low[b]	Low[b]	Low[b]	Low[b]	Low[b]
		Low[c]	Low[c]	Low[c]	Low[c]	Low[c]

Note: Classified in accordance with [a] Seed et al. (1962), [b] Holtz and Gibbs (1956), and [c] Sridharan and Prakash (2000).

the stabilization of an expansive soil from South Australia. In view of the test results and their interpretation, conclusions can be drawn as follows:

(1) All soil−PAM mixtures exhibited higher *LL*, *PL* and *PI* values compared to those obtained for the unamended soil. The greater the PAM dosage, the higher the *LL*, *PL* and *PI* parameters up to $P_D = 0.2$ g/L, beyond which only marginal variations occurred. On this basis, and particularly considering that higher dosages did not lead to notable further increases in the *LL*, it was speculated that the maximum tendency for clay particle flocculation occurs at 0.2 g/L PAM.

(2) All soil−PAM suspensions produced lower equilibrium sediment volumes (and hence lower *FSR* values) compared to that of the soil−water suspension. The *FSR* followed an exponentially-decreasing trend with increasing PAM dosage, although only minor added reductions were achieved beyond 0.2 g/L PAM, further confirming that this dosage produced the maximum tendency for flocculation.

(3) Because of their relatively higher viscosity compared to water, the use of PAM solutions as the compaction liquid induced inter-particle lubrication, thereby permitting a denser packing of the soil particles (and hence a higher MDUW) to be obtained. It was noted that the corresponding OMC values exhibited negligible changes in relation to the compacted unamended soil.

(4) Overall, the relative swelling and shrinkage strains decreased with increasing number of applied swell−shrink cycles, with
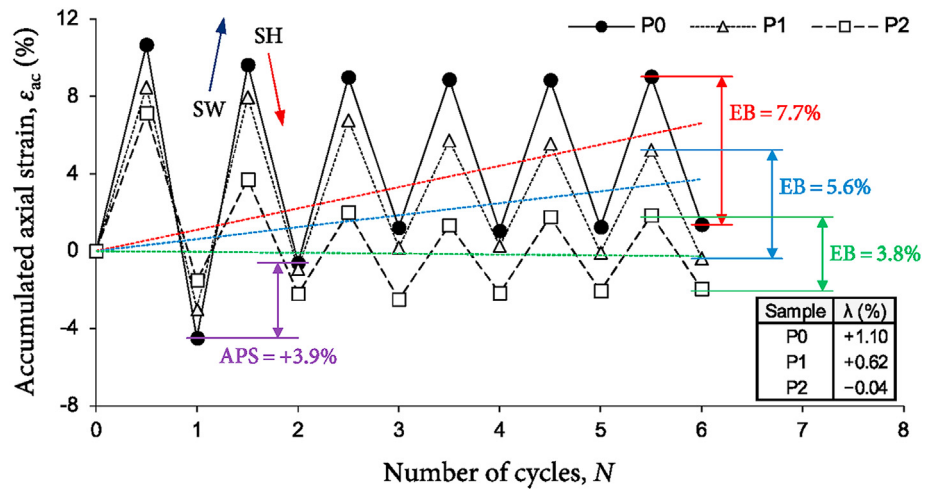
(a)
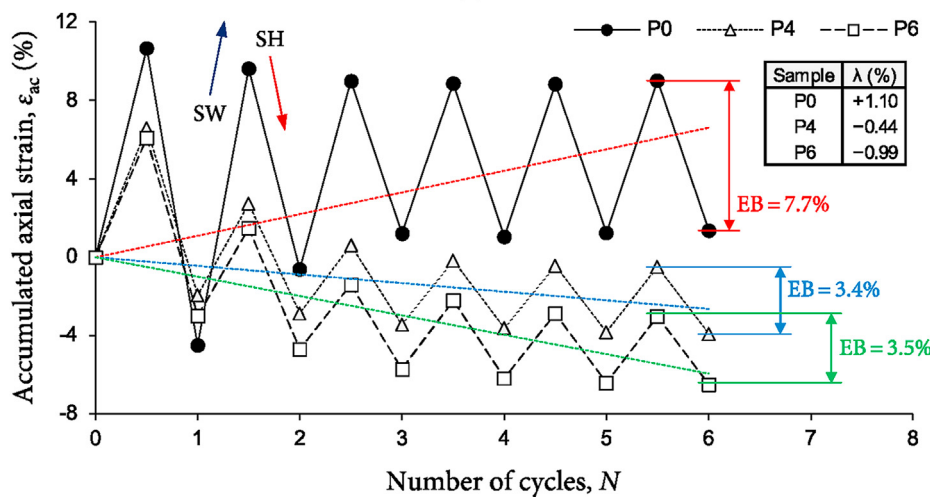
(b)

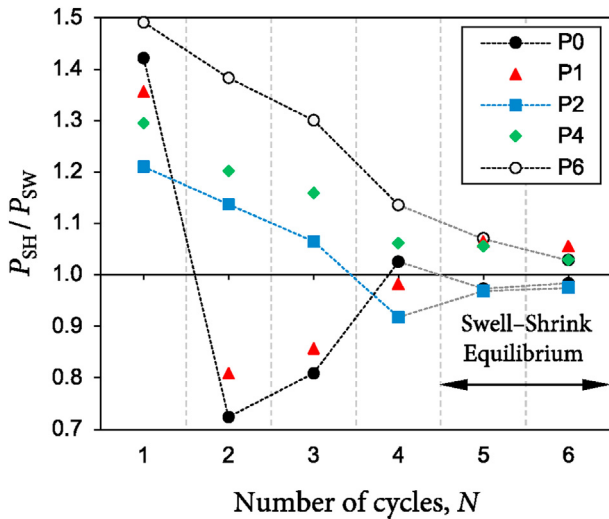**Fig. 6.** Cumulative swell−shrink patterns for the tested samples: (a) P0, P1 and P2; and (b) P0, P4 and P6.

Fig. 7. Variations of the shrinkage-to-swelling potential ratio (i.e. P_{SH}/P_{SW}) against the number of applied swell−shrink cycles N for the tested samples.

an 'elastic equilibrium' condition achieved on the conclusion of four cycles. The tendency for swelling/shrinkage potential reduction was found to be in favor of increasing the PAM dosage up to $P_D = 0.2$ g/L, beyond which the observed reductions became marginal. It was postulated that increasing the PAM dosage beyond 0.2 g/L can cause the excess PAM molecules to function as a lubricant instead of a flocculant; thence, this critical dosage was termed MFD.

(5) With PAM addition, the accumulated axial strain progressively transitioned from expansive for the unamended soil to neutral at $P_D = 0.2$ g/L, while higher PAM dosages of 0.4 g/L and 0.6 g/L both demonstrated undesirable contractive states. Based on these results, 0.2 g/L PAM, which also happens to represent the soil's MFD, was deemed as the optimum dosage in terms of minimizing swell−shrink-induced heave and settlements.

Unlike traditional calcium-based binders, which can be optimized in terms of dosage (or mix design) by simple standardized laboratory tests (e.g. pH measurements for soil−lime mixtures) based on an extensive body of knowledge built up over the years, no such framework has been developed (nor suggested) for PAM-based materials. From this experimental study, it can be hypothesized that basic geotechnical laboratory tests, such as consistency limits and sediment volume tests, can be used to predict the MFD for PAM-treated expansive clayey soils (i.e. without the need for conducting more advanced oedometer tests). Additional tests, employing different types of clayey soils with varying mineralogical and plasticity characteristics, should be performed with the aims of (i) further exploring potential correlations between the MFD and fundamental clay properties, and (ii) establishing a universal test framework capable of quantifying the MFD in a practical manner.

Declaration of competing interest

The authors declare that they have no known competing financial interests or personal relationships that could have appeared to influence the work reported in this paper.

Acknowledgments

Abbreviations

AMD	Acrylamide
APS	Axial plastic strain
AS	Australian Standard
ASTM	American Society for Testing and Materials
CH	High-plasticity clay
EB	Equilibrium bandwidth
FSR	Free swell ratio
LL	Liquid limit
MDUW	Maximum dry unit weight
MFD	Maximum flocculation dosage (for PAM)
OMC	Optimum moisture content
P0	Unamended soil
P1	Soil stabilized with 0.1 g/L PAM
P2	Soil stabilized with 0.2 g/L PAM
P4	Soil stabilized with 0.4 g/L PAM
P6	Soil stabilized with 0.6 g/L PAM
PAM	Polyacrylamide
PI	Plasticity index
PL	Plastic limit
SH	Shrinkage
SP	Standard Proctor
SW	Swelling

References

Al-Taie, A., Disfani, M., Evans, R., Arulrajah, A., 2020. Effect of swell−shrink cycles on volumetric behavior of compacted expansive clay stabilized using lime. Int. J. GeoMech. 20, 04020212.

AS 1289.3.2.1, 2009. Methods of Testing Soils for Engineering Purposes: Soil Classification Tests — Determination of the Plastic Limit of a Soil — Standard Method. Standards Australia (SA), Sydney, NSW, Australia.

AS 1289.3.4.1, 2008. Methods of Testing Soils for Engineering Purposes: Soil Classification Tests — Determination of the Linear Shrinkage of a Soil — Standard Method. Standards Australia (SA), Sydney, NSW, Australia.

AS 1289.3.9.1, 2015. Methods of Testing Soils for Engineering Purposes: Soil Classification Tests — Determination of the Cone Liquid Limit of a Soil. Standards Australia (SA), Sydney, NSW, Australia.

ASTM D2487-17, 2017. Standard Practice for Classification of Soils for Engineering Purposes (Unified Soil Classification System). ASTM International, West Conshohocken, PA, USA.

ASTM D422-63(2007)e2, 2007. Standard Test Method for Particle-Size Analysis of Soils. ASTM International, West Conshohocken, PA, USA.

ASTM D4546-14, 2014. Standard Test Methods for One-Dimensional Swell or Collapse of Soils. ASTM International, West Conshohocken, PA, USA.

ASTM D698-12, 2012. Standard Test Methods for Laboratory Compaction Characteristics of Soil Using Standard Effort (12400 ft-lbf/ft3 (600 kN-m/m3. ASTM International, West Conshohocken, PA, USA.

ASTM D854-14, 2014. Standard Test Methods for Specific Gravity of Soil Solids by Water Pycnometer. ASTM International, West Conshohocken, PA, USA.

Barvenik, F.W., 1994. Polyacrylamide characteristics related to soil applications. Soil Sci. 158, 235−243.

Ben-Hur, M., Malik, M., Letey, J., Mingelgrin, U., 1992. Adsorption of polymers on clays as affected by clay charge and structure, polymers properties, and water quality. Soil Sci. 153, 349−356.

Chang, I., Lee, M., Tran, A.T.P., Lee, S., Kwon, Y.M., Im, J., Cho, G.C., 2020. Review on biopolymer-based soil treatment (BPST) technology in geotechnical engineering practices. Transp. Geotech. 24, 100385.

Consoli, N.C., Araújo, M.T.D., Ferrazzo, S.T., Rodrigues, V.D.L., Rocha, C.G.D., 2021. Increasing density and cement content in expansive soils stabilization: conflicting or complementary procedures for reducing swelling? Can. Geotech. J. 58 (6).

Estabragh, A.R., Parsaei, B., Javadi, A.A., 2015. Laboratory investigation of the effect of cyclic wetting and drying on the behaviour of an expansive soil. Soils Found. 55, 304−314.

Estabragh, A.R., Soltani, A., Javadi, A.A., 2020. Effect of pore water chemistry on the behaviour of a kaolin−bentonite mixture during drying and wetting cycles. Eur. J. Environ. Civ. Eng. 24, 895−914.

Garzón, E., Cano, M., O'Kelly, B.C., Sánchez-Soto, P.J., 2015. Phyllite clay–cement composites having improved engineering properties and material applications. Appl. Clay Sci. 114, 229–233.

Georgees, R.N., Hassan, R., 2020. Performance-related properties of low-volume roads when stabilised with a sustainable anionic polyacrylamide: particle and specimen-levels study. Road Mater. Pavement Des. https://doi.org/10.1080/14680629.2020.1831945.

Gurtug, Y., Sridharan, A., 2002. Prediction of compaction characteristics of fine-grained soils. Geotechnique 52, 761–763.

Gurtug, Y., Sridharan, A., 2004. Compaction behaviour and prediction of its characteristics of fine grained soils with particular reference to compaction energy. Soils Found. 44, 27–36.

Holtz, W.G., Gibbs, H.J., 1956. Engineering properties of expansive clays. Trans. Am. Soc. Civ. Eng. 121, 641–663.

Ikeagwuani, C.C., Nwonu, D.C., 2019. Emerging trends in expansive soil stabilisation: a review. J. Rock Mech. Geotech. Eng. 11, 423–440.

James, J., 2020. Sugarcane press mud modification of expansive soil stabilized at optimum lime content: strength, mineralogy and microstructural investigation. J. Rock Mech. Geotech. Eng. 12, 395–402.

Jones, L.D., Jefferson, I., 2012. Expansive soils. In: Burland, J., Chapman, T., Brown, M., Skinner, H. (Eds.), ICE Manual of Geotechnical Engineering, vol. I. ICE Publishing, London, UK, pp. 413–441.

JTG E40-07, 2007. Test Methods of Soils for Highway Engineering. The Ministry of Transport of the People's Republic of China (MOT), Beijing, China.

Kalkan, E., 2011. Impact of wetting–drying cycles on swelling behavior of clayey soils modified by silica fume. Appl. Clay Sci. 52, 345–352.

Khatami, H.R., O'Kelly, B.C., 2013. Improving mechanical properties of sand using biopolymers. J. Geotech. Geoenviron. Eng. 139, 1402–1406.

Kim, S., Palomino, A.M., 2009. Polyacrylamide-treated kaolin: a fabric study. Appl. Clay Sci. 45, 270–279.

Kou, H.L., Jia, H., Chu, J., Zheng, P.G., Liu, A.S., 2021. Effect of polymer on strength and permeability of marine clay. Mar. Georesour. Geotechnol. 39, 234–240.

Laird, D.A., 1997. Bonding between polyacrylamide and clay mineral surfaces. Soil Sci. 162, 826–832.

Latifi, N., Rashid, A.S.A., Siddiqua, S., Majid, M.Z.A., 2016. Strength measurement and textural characteristics of tropical residual soil stabilised with liquid polymer. Measurement 91, 46–54.

Lei, H., Xu, Y., Li, X., Zheng, G., Liu, G., 2018. Effects of polyacrylamide on the consolidation behavior of dredged clay. J. Mater. Civ. Eng. 30, 04018022.

Lu, J.H., Wu, L., Letey, J., 2002. Effects of soil and water properties on anionic polyacrylamide sorption. Soil Sci. Soc. Am. J. 66, 578–584.

Mirzababaei, M., Yasrobi, S.S., Al-Rawas, A.A., 2009. Effect of polymers on swelling potential of expansive soils. Proc. Inst. Civ. Eng. – Gr. Improv. 162, 111–119.

Muguda, S., Nagaraj, H.B., 2019. Effect of enzymes on plasticity and strength characteristics of an earthen construction material. Int. J. Geo-Eng. 10, 2.

Onyejekwe, S., Ghataora, G.S., 2015. Soil stabilization using proprietary liquid chemical stabilizers: sulphonated oil and a polymer. Bull. Eng. Geol. Environ. 74, 651–665.

Orts, W.J., Roa-Espinosa, A., Sojka, R.E., Glenn, G.M., Imam, S.H., Erlacher, K., Pedersen, J.S., 2007. Use of synthetic polymers and biopolymers for soil stabilization in agricultural, construction, and military applications. J. Mater. Civ. Eng. 19, 58–66.

Prakash, K., Sridharan, A., 2004. Free swell ratio and clay mineralogy of fine-grained soils. Geotech. Test J. 27, 220–225.

Seed, H.B., Woodward, J., Lundgren, R., 1962. Prediction of swelling potential for compacted clays. J. Soil Mech. Found Div. 88, 53–87.

Seybold, C.D., 1994. Polyacrylamide review: soil conditioning and environmental fate. Commun. Soil Sci. Plant Anal. 25, 2171–2185.

Sivapullaiah, P.V., 2015. Surprising soil behaviour: is it really!!! Indian Geotech. J. 45, 1–24.

Soltani, A., Deng, A., Taheri, A., Mirzababaei, M., 2018. Rubber powder–polymer combined stabilization of South Australian expansive soils. Geosynth. Int. 25, 304–321.

Soltani, A., Deng, A., Taheri, A., O'Kelly, B.C., 2019a. Engineering reactive clay systems by ground rubber replacement and polyacrylamide treatment. Polymers 11, 1675.

Soltani, A., Deng, A., Taheri, A., Mirzababaei, M., 2019b. A sulphonated oil for stabilisation of expansive soils. Int. J. Pavement Eng. 20, 1285–1298.

Soltani, A., Deng, A., Taheri, A., Mirzababaei, M., Vanapalli, S.K., 2019c. Swell–shrink behavior of rubberized expansive clays during alternate wetting and drying. Minerals 9, 224.

Soltani, A., Taheri, A., Deng, A., O'Kelly, B.C., 2020a. Improved geotechnical behavior of an expansive soil amended with tire-derived aggregates having different gradations. Minerals 10, 923.

Soltani, A., Taheri, A., Deng, A., Nikraz, H., 2020b. Tyre rubber and expansive soils: two hazards, one solution. Proc. Inst. Civ. Eng. – Constr. Mater. https://doi.org/10.1680/jcoma.18.00075.

Soltani, A., Raeesi, R., O'Kelly, B.C., 2021. Cyclic swell–shrink behaviour of an expansive soil treated with a sulfonated oil. Proc. Inst. Civ. Eng. – Gr. Improv. https://doi.org/10.1680/jgrim.19.00084.

Soltani-Jigheh, H., Bagheri, M., Amani-Ghadim, A.R., 2019. Use of hydrophilic polymeric stabilizer to improve strength and durability of fine-grained soils. Cold Reg. Sci. Technol. 157, 187–195.

Sridharan, A., Prakash, K., 1999. Influence of clay mineralogy and pore-medium chemistry on clay sediment formation. Can. Geotech. J. 36, 961–966.

Sridharan, A., Prakash, K., 2000. Classification procedures for expansive soils. Proc. Inst. Civ. Eng. Geotech. Eng. 143, 235–240.

Subba Rao, K.S., 2000. Swell–shrink behaviour of expansive soils — geotechnical challenges. Indian Geotech. J. 30, 1–68.

Theng, B.K.G., 1982. Clay–polymer interactions: summary and perspectives. Clay Clay Miner. 30, 1–10.

Thyagaraj, T., Zodinsanga, S., 2014. Swell–shrink behaviour of lime precipitation treated soil. Proc. Inst. Civ. Eng. – Gr. Improv. 167, 260–273.

Tripathy, S., Subba Rao, K.S., Fredlund, D.G., 2002. Water content–void ratio swell–shrink paths of compacted expansive soils. Can. Geotech. J. 39, 938–959.

Vardanega, P.J., O'Kelly, B.C., Haigh, S.K., 2020. Discussion of "reclaimed lignin-stabilized silty soil: undrained shear strength, atterberg limits, and microstructure characteristics". In: Zhang, Tao, Cai, Guojun, Liu, Songyu (Eds.), Journal of Materials in Civil Engineering, 32, 07020001, 3.

Xiong, B., Loss, R.D., Shields, D., Pawlik, T., Hochreiter, R., Zydney, A.L., Kumar, L., 2018. Polyacrylamide degradation and its implications in environmental systems. npj Clean Water 1, 17.

Yazdandoust, F., Yasrobi, S.S., 2010. Effect of cyclic wetting and drying on swelling behavior of polymer-stabilized expansive clays. Appl. Clay Sci. 50, 461–468.

Zhang, R., Yang, H., Zheng, J., 2006. The effect of vertical pressure on the deformation and strength of expansive soil during cyclic wetting and drying. In: Miller, G.A., Zapata, C.E., Houston, S.L., Fredlund, D.G. (Eds.), Unsaturated Soils 2006. ASCE, Reston, VA, USA, pp. 894–905.

Zhang, T., Deng, Y., Lan, H., Zhang, F., Zhang, H., Wang, C., Tan, Y., Yu, R., 2019. Experimental investigation of the compactability and cracking behavior of polyacrylamide-treated saline soil in Gansu Province, China. Polymers 11, 90.

Zhang, J., Deng, A., Jaksa, M., 2021. Optimizing micaceous soil stabilization using response surface method. J. Rock. Mech. Geotech. Eng. 13 (1), 212–220.

Zhao, N.F., Ye, W.M., Chen, Y.G., Chen, B., Cui, Y.J., 2019. Investigation on swelling–shrinkage behavior of unsaturated compacted GMZ bentonite on wetting–drying cycles. Bull. Eng. Geol. Environ. 78, 617–627.

Dr. Amin Soltani is a Lecturer of civil engineering in the School of Engineering, IT and Physical Sciences at Federation University Australia. He also holds an honorary affiliation with the University of Melbourne. Dr. Soltani completed his PhD degree at the University of Adelaide, Australia in 2018. Prior to his current appointment, he was a Research Fellow in geotechnical engineering at the University of Melbourne and University of Adelaide, where he played a significant leading role in the advancement of numerous research projects in collaboration with reputable industry partners, city councils, and governmental agencies. His principal research interests lie in the fields of experimental geomechanics and transportation/pavement geotechnics. An exciting aspect of his research, which is mainly interdisciplinary, involves reusing solid waste materials and industrial by-products, in conjunction with emerging trends in geotechnical engineering such as polymer technology, to develop new and sustainable geomaterials.